ACADEMIA ROMÂNĂ
Revue Roumaine de Chimie
http://web.icf.ro/rrch/

Rev. Roum. Chim.,
2011, *56*(6), 589-593

RIETVELD REFINEMENT OF POWDER X-RAY DIFFRACTION OF NANOCRYSTALLINE NOBLE METALS – TUNGSTEN TRIOXIDE

Emil INDREA,[a]* Ecaterina BICA,[b] Elisabeth-Jeanne POPOVICI,[b] Ramona-Crina SUCIU,[a]
Marcela Corina ROŞU[a] and Teofil-Dănuț SILIPAŞ[a]

[a] National Institute for Research and Development of Isotopic and Molecular Technologies, 65-103 Donath, RO-400293, Cluj-Napoca, Roumania
[b] "Raluca Ripan" Institute for Research in Chemistry, Babeş-Bolyai University, 30 Fântanele, Cluj-Napoca, Roumania

Recieved November 5, 2010

Tungsten trioxide powders were prepared from peroxo-tungstic acid (PTA) precursor obtained by sol-gel route, in aqueous medium. Two WO_3 samples were doped with noble metals, by "loading" them with silver and metallic palladium. The unit cell parameters of the WO_3 monoclinic phase, the effective crystallite mean size, D_{eff} (nm), and the mean root mean square (rms) of the microstrains , $\langle \varepsilon^2 \rangle^{1/2}_{hkl}$,were calculated by Rietveld refinement analysis. The distorsion of the WO_3 crystal structure has been used by the ISODISPLACE software tool to transform the *P*2_1/*n* structure of WO_3 on to the distortion-mode basis to visualize and quantify the displace modes. The atomic coordinate type has been used to compute three-dimensional structure model as the Radial Distribution Functions g(r) for a 3000-atom model of WO_3-Ag and WO_3-Pd systems, which reflects the space correlations between W-O and W-W atoms.

INTRODUCTION

Tungsten oxide (WO_3) is a wide-band gap semiconductor of great interest because of its applications in optoelectronics, catalysis and environmental engineering.[1] Application of tungsten trioxide strongly depends on morpho-structural characteristics that are regulated during the synthesis.

Tungsten trioxide could be obtained by different preparation methods such as precipitation, sol-gel, hydrothermal, etc. Among these, the sol-gel, inorganic route offers the advantage of being an inexpensive synthesis method that allows the control of powders properties with homogeneous crystalline structure and nanosized particles. Due to their nanostructured and surface area properties, WO_3 powders can be used as photocatalysts for dye degradation in waste waters. The photocatalytic activity of WO_3 powders could be improved by their "doping" with metals or metallic oxides.[2,3]

The goal of the study is to investigate the structural properties of WO_3 nanopowders "loaded" with precious metals that are supposed to improve their photocatalytic activity. The influence of silver and palladium on the crystalline parameters of tungsten trioxide is investigated.

EXPERIMENTAL

Tungsten trioxide powders were prepared from peroxo-tungstic acid (PTA) precursor obtained by sol-gel route, in aqueous medium, by dissolving tungsten powder (Merck) in hydrogen peroxide (30%, Merck) and drying the clear yellow solution at 70°C. The obtained precursor was annealed at 550°C, for 30 minutes, in air, to give the WO_3 sample.[4,5]

Two WO_3 samples were doped with noble metals, by "loading" them with silver (nominated WO_3-Ag) and metallic palladium (nominated WO_3-Pd), respectively. WO_3-Ag sample was prepared by impregnating the PTA precursor with silver nitrate and its annealing at 550°C. WO_3-Pd sample was obtained by coating the WO_3 powder grains with palladium nanoparticles and drying them at 110°C. Undoped WO_3 (sample WO_3) under-micron powder were prepared from

* Corresponding author: emil.indrea@itim-cj.ro

peroxotungstic acid (PTA) precursor obtained by sol-gel route, in aqueous medium (W pwd. dissolution in H_2O_2, WO_3-SG sample).

X-ray diffraction (XRD) measurements were performed using a BRUKER D8 Advance X-ray diffractometer, working at 40 kV and 40 mA with a germanium monochromator in the incident beam. The X-ray diffraction patterns were collected in a step-scanning mode with steps of $\Delta 2\theta = 0.01°$ using Cu Kα1 radiation (λ = 1.54056 Å) in the 2θ range 15-85°. Pure corundum powder standard sample was used to correct the data for instrumental broadening.

XRD patterns of the investigated samples were used for crystal phase analysis. Phase analysis was carried out using the using PDF and wo3_iso.cif files and unit cell parameters were calculated through structure Rietveld refinement. In the Rietveld analysis, we employed the program MAUDWEB 2.062.[6] It is designed to refine simultaneously both the structural (lattice cell constants, atomic positions and occupancies) and microstructural parameters (crystallite size and r.m.s. strain).

RESULTS AND DISCUSSION

XRD diffraction patterns (Fig. 1) illustrate the fact that all samples obtained in our synthesis conditions are WO_3 monoclinic crystalline structure phase (PDF file # 83-0951).

The Rietveld refinement of the X-ray diffraction data has been done using the JAVA based software namely Materials Analysis Using Diffraction (MAUD). [6]

The MAUD software can effectively characterize the material which contain anisotropy of size and strain which causes the diffraction profiles to broaden. The effective crystallite size (D_{eff}) and the root mean square microstrain ($<\varepsilon^2>^{1/2}$) were evaluated using the Popa model.[7]

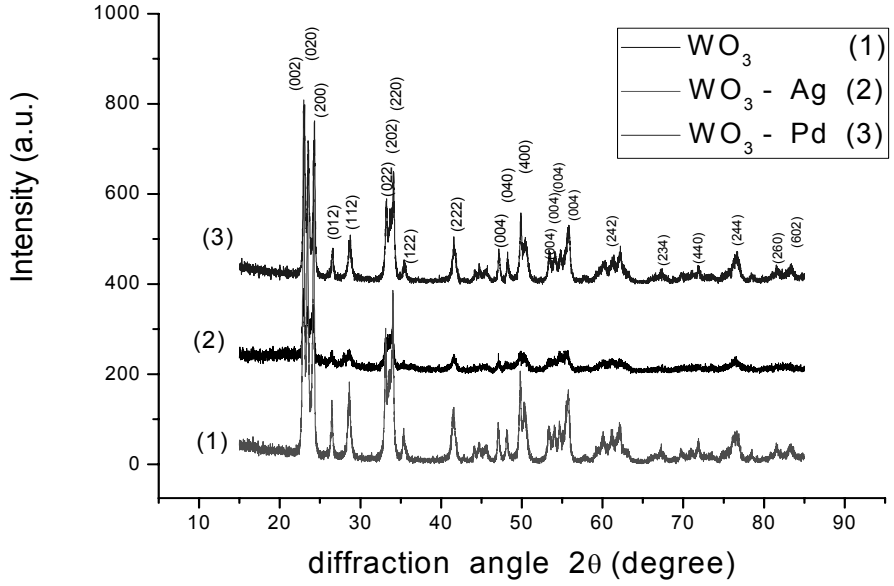

Fig. 1 – X-ray diffraction patterns of the WO_3, WO_3-Ag and WO_3-Pd samples.

In the present study, instrumental broadening part was incorporated in the Rietveld analysis. The instrumental resolution parameters for peak asymmetry, instrumental broadening, etc. were calculated from the corundum standard powder. To simulate the X-ray powder diffraction patterns of WO_3 monoclinic phase, the following input parameters were used: WO_3 monoclinic crystal system, space group: **P2_1/n** (SG 14) (PDF file # 83-0951) and W^{VI} and O^{2-} in special Wyckoff positions at 4e.[8]

The structural parameters of WO_3 phase at room temperature are presented in the Table 1.

Table 1

The structural parameters of WO_3-phase **P2_1/n** (SG 14) at room temperature[8]

Atoms	x	y	z	Atoms	x	y	z
W1	0.2513(6)	0.0277(7)	0.2865(5)	O3	0.2821(4)	0.2602(7)	0.2870(4)
W2	0.2481(6)	0.0342(6)	0.7815(5)	O4	0.2107(4)	0.2602(8)	0.7310(4)
O1	0.0008(6)	0.0366(8)	0.2116(5)	O5	0.2859(6)	0.0390(6)	0.0065(5)
O2	0.9973(6)	0.4632(8)	0.2164(5)	O6	0.2849(6)	0.4850(5)	0.9922(4)

a = 7.30084(7) Å , b = 7.53889(7) Å , c = 7.68962(8) Å, β = 90.892(1)

The background of each pattern was fitted by a fourth order polynomial function. First, the background was refined; the positions of the peaks were corrected for zero-shift error by successive refinements and then the structural and microstructural parameters were refined. The unit cell parameters of the WO_3 monoclinic phase, the effective crystallite mean size, D_{eff} (nm), and the mean root mean square (rms) of the microstrains, $\langle\varepsilon^2\rangle^{1/2}_{hkl}$, calculated by Rietveld refinement analysis using MAUD computer program are presented in Table 2.

Microstructural parameters *i.e.* the effective crystallite mean size and the root mean square of the microstrains illustrate the accommodation of Ag atoms into the monoclinic WO_3 structure. The microcrystalline strain is stronger for WO_3-Ag sample and that is based on higher disordered host lattice (due to the Ag atoms substitution), constituted from smaller crystallites (48 nm). In contrast, there are relatively few lattice faults in WO_3 and WO_3-Pd crystals that are built from relatively larger crystallites (82-93 nm). The unit cell volume of WO_3-Ag sample is larger over WO_3 sample, thus suggesting a more disordered atom packing in Ag-doped WO_3 monoclinic lattice.

Typical Rietveld refinement plot for X-ray diffraction pattern of the WO_3-Pd sample is presented in Fig. 2a. The fractional atomic coordinates and Debye-Waller isotropic temperature factor for the WO_3-Pd sample are presented in Fig. 2b.

Table 2

The unit cell parameters of the WO_3 monoclinic phase, the effective crystallite mean size, D_{eff} (nm), the mean root mean square (rms) of the microstrains , $\langle\varepsilon^2\rangle^{1/2}_{hkl}$ and profile (Rp) discrepancy indices calculated by Rietveld refinement analysis for WO_3, WO_3-Pd and WO_3-Ag samples

Samples	a [nm]	b [nm]	c [nm]	beta [deg.]	V × 10^3 [nm]^3	D_{eff} [nm]	$\langle\varepsilon^2\rangle^{1/2}_{hkl}$ × 10^3	R_p
WO_3	0.7325(9)	0.7548(9)	0.7709(7)	90.53(7)	0.4263(5)	93.(3)	1.11(2)	12.2
WO_3-Ag	0.7329(3)	0.7549(7)	0.7713(1)	90.57(4)	0.4267(8)	48.(0)	2.22(4)	14.6
WO_3-Pd	0.7326(1)	0.7549(1)	0.7711(8)	90.54(1)	0.4264(9)	82.(8)	0.98(7)	11.2

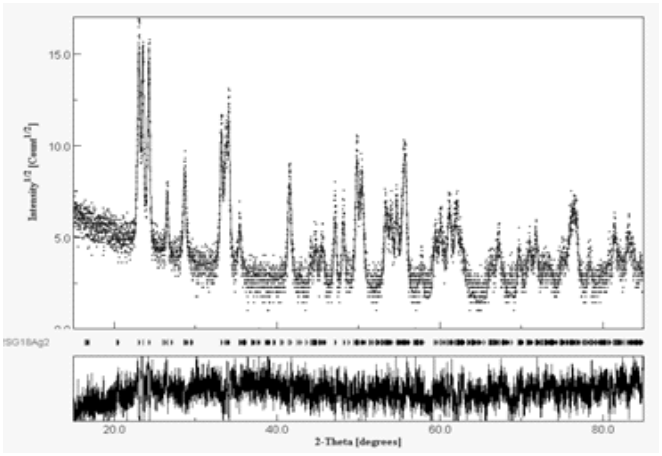

a

Distorted superstructure (14 P2_1/n)
a=7.3493(8) Å , b=7.5356(8) Å , c=7.7081(8)Å,
alpha=90.00, beta=89.40(8), gamma=90.00

atom	site	x	y	z	B_{iso} [Å^2]
W1	4e	0.25(6)	0.02(0)	0.28(0)	0.27(8)
W2	4e	0.23(9)	0.03(4)	0.78(2)	0.36(2)
O1	4e	0.00(9)	0.04(6)	0.21(8)	0.42(9)
O2	4e	0.02(7)	0.39(8)	0.25(8)	0.79(3)
O3	4e	0.29(7)	0.27(8)	0.29(2)	0.52(2)
O4	4e	0.24(2)	0.28(0)	0.68(1)	0.56(6)
O5	4e	0.30(2)	0.00(4)	0.03(9)	0.49(3)
O6	4e	0.28(7)	0.53(0)	0.02(5)	0.40(9)

Sample WO_3-Pd

b

Fig. 2 – (a) Typical refinement plot for X-ray diffraction pattern of the WO_3-Pd sample. The experimental diffraction pattern is described by symbols and the refined one with a continuous line. The quality of the refinement is shown by the difference between both patterns, which correspond to the curve at the bottom of the figure; (b) The *P2_1/n* monoclinic structure of WO_3-Pd at room temperature.

In order to investigate the distorsion of the WO_3 crystal structure we have used the ISODISPLACE software tool[9,10] to transform the *P2_1/n* structure of WO_3-Pd and WO_3-Ag systems onto the distortion-mode basis to visualize and quantify the displacive modes that give rise to this distortions (Fig. 3(a)-(c)). ISODISPLACE is a tool for exploring the structural distortion modes of crystalline materials.

Given parent-phase structural information, it generates atomic displacement patterns induced by irreducible representations of the parent space-group symmetry starting from fractional atomic coordinates of individual phases and allows a user to visualize and manipulate the amplitude of each distortion mode interactively. ISODISPLACE uses the subroutines of the ISOTROPY software suite to generate atomic displacement patterns induced by representations of the parent space-group symmetry at reciprocal-space ***k*** points. The distorted *P2_1/n* structure file named wo3_iso.cif. contain in addition to the traditional atomic-coordinate description of the distorted structure, the complete distortion-mode description. This file also includes other information that structure-refinement packages will need in order to directly refine the distortion-mode amplitudes. These are (1) the atomic coordinate shifts, which all equal zero in the undistorted parent phase, (2) the formula relationships between the distorted atomic coordinates, undistorted coordinates and coordinate shifts, and (3) the 24×24 matrix (in sparse form) that transforms the distortion-mode amplitudes into the coordinate shifts.

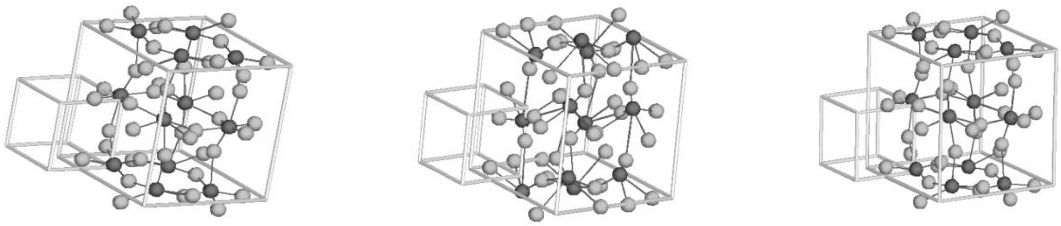

a-WO_3 **b-WO_3-Pd** **-WO_3-Ag**

Fig. 3 – Comparison of P2_1/n structure of WO_3 and a structure described by distorsion modes. Atomic coordinates coordinates are shown in distortion-mode structure in green (W atoms) and red (O atoms). The distorsion of the WO_3 crystal structure (a) and the distorsion of WO_3-Pd (b) and WO_3-Ag (c) systems are presented onto the distortion-mode basis to visualize and quantify the displacive modes.

Detailed information calculated through Rietveld refinement using the MAUD and ISODISPLACE softwares about the atomic coordinate type (e.g. Cartesian or fractional) has been used to compute three-dimensional structure model as the Radial Distribution Functions g(r) (RDF)[11,12] by a computer program named ISAACS.[9] The structure of disordered materials can only be quantitatively described in terms of the radial distribution function g(r), indicating the average probability of finding another atom in a specified volume from an origin atom as a function of radial distance. Detailed knowledge about the three-dimensional atomic scale structure is a prerequisite to understanding and predicting properties of materials. The models need to be analyzed further so that important details of the atomic scale structure, such as distribution of first atomic neighbors, bond angles and local symmetry, are well understood.

Results of the calculation of the radial distribution functions RDF for a 3000-atom model of WO_3-Pd and WO_3-Ag (see Fig. 4) systems exhibits a first group of peaks (1.3 – 2.3 Å) that reflects the correlations between W1-O4, W1-O1, W1-O3, W2-O6 and W1-O5 atoms and a second group positioned around 3.8 Å, that reflects the correlations between W1-W2 atoms. The local O neighborhood of W ions is strongly disordered in the WO_3-Ag photocatalyst, with appreciable non-Gaussian contribution to the RDF. The second RDF peak in the WO_3-Ag photocatalyst corresponds mainly to W1-W2 interatomic distance centered around 3.8 Å is also distorted (both peaks strongly overlap) confirming the Ag atoms substitution process in the WO_3 monoclinic lattice.

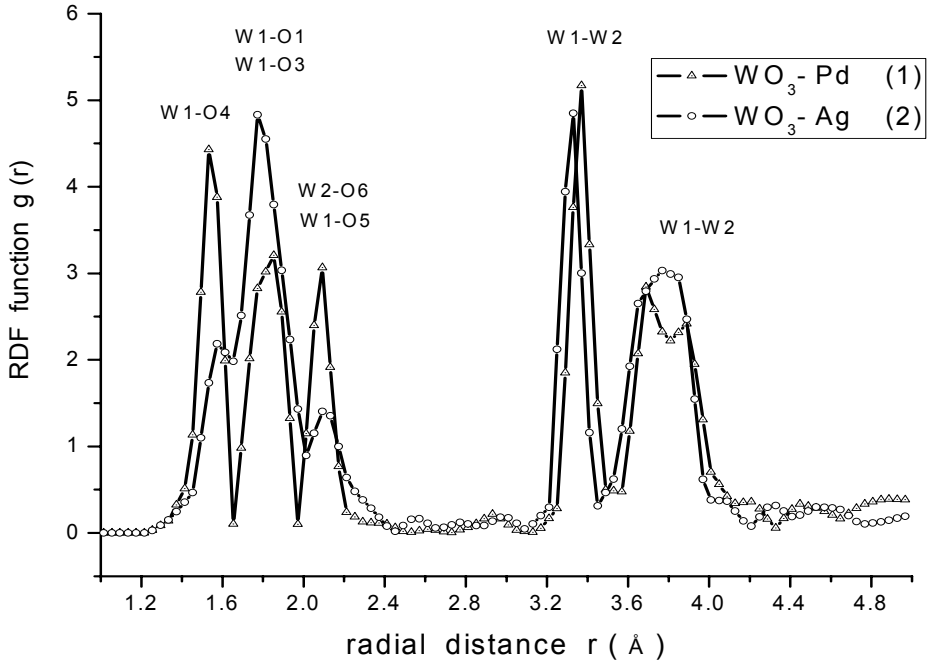

Fig. 4 – RDF for a 3000-atom model of WO_3-Pd and WO_3-Ag photocatalysts.

The photocatalytic activity of WO_3, WO_3-Pd and WO_3–Ag powders was determined for the degradation of azo-dyes. It was revealed that the "coating" of WO_3 particles with palladium nanoclusters (WO_3-Pd; extra-grains metal "doping") increases the photocatalytic efficiency with 46% whereas the loading of WO_3–Ag powder with silver (WO_3–Ag; intra-grain metal "doping") decreases it with 25%, in comparison with the un-doped WO_3 powder.

CONCLUSIONS

XRD diffraction patterns illustrate the fact that all samples obtained in our synthesis conditions are WO_3 monoclinic crystalline structure phase.

Microstructural parameters *i.e.* the effective crystallite mean size and the root mean square of the microstrains illustrate the accommodation of Ag atoms into the monoclinic WO_3 structure.

Detailed information calculated through Rietveld refinement using the MAUD software about the atomic coordinate type has been used to compute three-dimensional structure model as the Radial Distribution Functions g(r) for a 3000-atom model of WO_3-Pd and WO_3-Ag systems, which reflects the space correlations between W-O and W-W atoms.

Acknowledgements: This work was supported by the Roumanian Ministry of Education and Research through the project INCDTIM Cluj-Napoca, PN 09-44 02 06.

REFERENCES

1. S. Wang, X. Shi, G. Shao, S. Duan, H. Yang and T. Wang, *J. Phys. Chem. Solid*., **2008**, *69*, 2396-2403.
2. M. A. Gondal, A. Bagabas, A. Dastageer and A. Khalil, *J Mol. Cata. A-Chem,* **2010**, *323*, 78-83.
3. T. Huang, X. Lin, J. Xing, W. Wang, Z. Shan and F. Huang, *Mater. Sci. & Eng. B*, **2007**, *141*, 49–54.
4. M. Ştefan, E. Bica, L. Muresan, R. Grecu, E. Indrea, M. Trif and E. J. Popovici, *J. Optoelectron. Adv. Mat., – Symposia,* **2010**, *2*, 115-118.
5. E. Bica, E.-J. Popovici, M. Ştefan, I. Perhaiţă and I. C. Popescu, *Stud. Univ. "Babeş-Bolyai", Chem,* XLV, **2010**, *2*, 169-177.
6. L. Lutterotti, MAUD Version 2.062, http://www.ing.unitn.it/_maud/**2007**.
7. N.C. Popa, *J. Appl. Crystallogr*., **1998**, *31*, 176-181.
8. P. M. Woodward, A. W. Sleight and T. Vogt, *J. Phys. Chem. Solids*, **1995**, *56,* 1305-1315.
9. S. Le Roux, V. Petkov, *J. Appl. Crystallogr*., **2010**, *43*, 181-185.
10. B. J. Campbell, H. T. Stokes, D. E. Tanner and D. M. Hatch, *J. Appl. Cryst*., **2006**, *39*, 607-614.
11. T. Petkova, M.Mitkova, Mir.Vlcek and S.Vassilev, *J.Non-Cryst.Solids*, **2003**,*327*,125-131.
12. N.E. Cusack, "The Physics of Structurally Disorder Matter", IOP Publishing Ltd., Bristol, England, 1987.